R&D OF SHORT-PERIOD NbTi AND Nb_3Sn SUPERCONDUCTING UNDULATORS FOR THE APS*

S.H. Kim†, C. Doose, R.L. Kustom, E.R. Moog and I. Vasserman
Advanced Photon Source, Argonne National Laboratory
9700 S. Cass Ave., Argonne, IL 60439, USA

Abstract

Superconducting undulators (SCUs) with a period of 14.5 mm are under development for the Advanced Photon Source (APS). The undulators have been designed to achieve a peak field on the beam axis higher than 0.8 T with an 8 mm pole gap and current densities over 1 kA/mm^2 in the NbTi and Nb_3Sn coils. Upper-half NbTi SCUs of short sections have been fabricated and were charged up to near the critical current density of 1.43 kA/mm^2 to achieve a peak field about 1 T. The stability margin of the SCU was measured by imposing steady-state heat fluxes on the pole/coil face of the SCU in a pool-boiling liquid He (LHe) dewar at 4.2 K. Near the critical current density, where the temperature stability margin is minimal, the heat flux density to quench the SCU was about 1.3 mW/mm^2, of which 60% was attributed to LHe at the interface of the SCU and the vacuum chamber. The peak fields of the SCU were mapped along the beam axis using a Hall probe in a vertical dewar. The first test of a Nb_3Sn short-section SCU was charged to an average current density of 1.45 kA/mm^2, slightly higher than the critical current density for the NbTi SCU.

INTRODUCTION

Short-period planar superconducting undulators (SCUs) are under development for the Advanced Photon Source (APS) [1]. The initial goal of the SCU program at the APS is to install a SCU with a tunable range of photon energy of the first harmonic from 19 to 29 keV in the APS 7-GeV storage ring (SR). Further extensions to this energy range can be achieved by using higher harmonics of the radiation when the device exhibits a high field quality, which would require detailed field mapping and tuning.

The design parameters of the undulator are a period λ of 14.5 - 15 mm and a peak field higher than 0.8 T on the beam axis for a pole gap g of at least 8 mm. This requires achieving an average current density in the superconducting (SC) coil over 1 kA/mm^2. The R&D efforts for the SCU have been mainly devoted to the developing SC coils for the device that achieve sufficiently high peak fields with good field uniformity.

This paper summarizes the current status of the design including magnetic aspects, fabrication of short-section NbTi SCUs, test results up to its critical current density, measurements of the thermal stability margins under pool boiling, magnetic field mapping, as well as the first test result of a Nb_3Sn short section.

*Work supported by the U.S. Department of Energy under Contract No. W-31-ENG-38.
†shkim@aps.anl.gov

FIELD CALCULATION AND DESIGN

The peak vertical field B_0 on the beam axis in the midplane of the SCU and the maximum field B_m in the coil were calculated as a function of the average current density in the coil. Figure 1 plots the calculated data for three pole gaps. Also plotted in the figure is the critical current density j_c(NbTi) as a function of B_m for the NbTi SC wire at 4.2 K. The average current density is limited to about 1.43 kA/mm^2 at 3.6 T. For a pole gap of 8 mm, the highest attainable B_0 on the beam axis would be about 1.0 T. For the three pole gaps, the coil maximum fields differ by less than 1%. The peak undulator field on the beam axis, on the other hand, depends significantly on the pole gap, as shown in Fig. 1. For a current density higher than 0.3 kA/mm^2, B_0 approximately follows a function of $\exp(-\pi g/\lambda)$ [2].

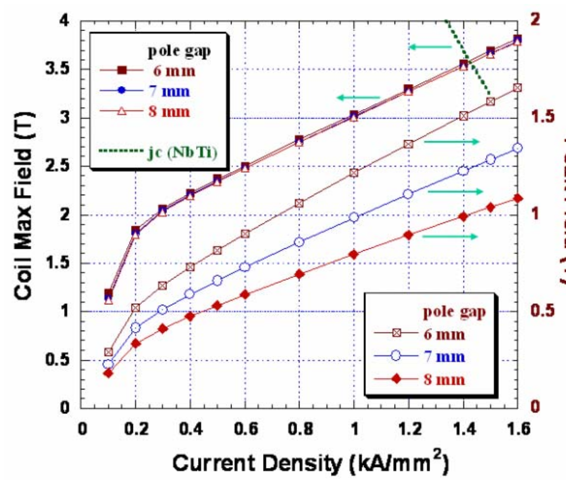

Figure 1: Calculated vertical peak field B_0 on the beam axis (*right axis*) and the coil maximum field B_m(coil) (*left axis*) for the SCU (λ = 15 mm) are plotted as a function of the coil average current density j. Also plotted are the critical current density j_c(NbTi) (*bottom axis*) of the SC coil B_m (*left axis*) at 4.2 K.

A 12-period core for upper-half NbTi SCUs (λ = 15 mm) was machined from "1008 low-carbon" steel. Another upper-half SCU (λ = 14.5 mm) with 22 periods was fabricated. The dimensions of the rectangular grooves for the coil windings in the core were 4.39 mm x 3.99 mm. Formvar-insulated NbTi SC wires with dimensions

0-7803-8859-3/05/$20.00 ©2005 IEEE

of 1.05 mm x 0.77 mm were used for the 20-turn coils per core groove. A 3.5-period core for a Nb_3Sn SCU (λ = 14.5 mm) had grooves 4.83 mm wide and 4.27 mm deep. A round Nb_3Sn SC wire with a bare diameter of 0.8 mm and glass insulation was used for 23-turn coils per groove.

THE PEAK FIELDS ACHIEVED

The two upper-half NbTi SCUs (λ = 15 mm and 14.5 mm) were tested at 4.2 K. The peak fields, B_0, were measured using a Hall probe at a fixed distance of approximately 3.6 mm from a magnetic pole face. The measured peak fields, as well as the calculated fields, are plotted in Fig. 2. Since the location of the Hall probe was not known accurately, the measured data were normalized to those of the calculations for the upper and lower halves of the SCUs with a pole gap of 8.0 mm. Because of the differences in the g/λ ratio between the two, the peak fields for the 15-mm SCU are higher compared to those for the 14.5-mm one by a factor of exp(π/54.4). When the SCUs were trained by means of quenches during the charging process, they nearly reached the critical current densities.

In the test of the upper-half short-section Nb_3Sn SCU, without any training it was charged up to a coil current density of 1.45 kA/mm^2, which is higher than the critical current density for the NbTi SCU. The corresponding peak field is about 0.98 T, as shown in Fig. 2. Subsequent trainings after the first quench did not increase the maximum current density any further.

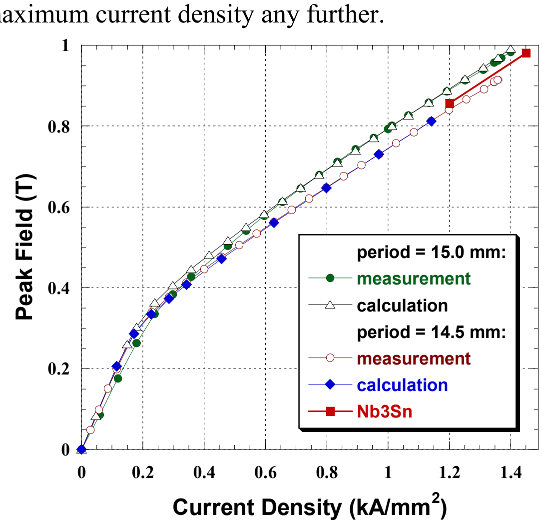

Figure 2: The peak fields B_0 for the two upper-half NbTi SCUs are plotted for a pole gap of 8 mm. The Nb_3Sn SCU (λ = 14.5 mm) reached a higher current density than that for the NbTi SCU.

STABILITY UNDER HEAT LOAD

Once the current density required to achieve the desired peak field is attained, the issue becomes one of stability at the operating current in the presence of the heat load from the electron beam and elsewhere. A test setup for the heat load is sketched in Fig. 3. A thin-film heater is attached to the 0.6-mm-thick inner wall of a vacuum chamber that presses against the coil/pole face. The heater has a cross section of 121 mm x 11 mm and a thickness of about 0.2 mm including thin insulation on both sides. The SCU axis was in the vertical direction during the test in a pool-boiling liquid He (LHe) dewar at 4.2 K.

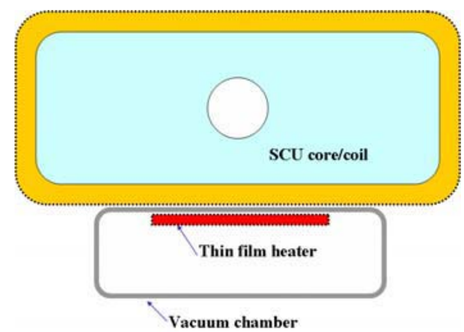

Figure 3: A 2-D sketch of the setup for the heat-load tests in a plane perpendicular to the undulator axis. A thin-film heater was attached to the inner wall of a vacuum chamber, which was attached to the SCU core/coil flat face.

The steady-state heat flux densities were measured when the SCU quenched. The measurements data are plotted in Fig. 4 for three different cases, two with LHe at the interface between the chamber and the SCU coil/pole face and one without it. Since the temperature margin between 4.2 K and the quench or current-sharing temperature should increase from zero at j_c to about 5 K at zero current, the flux densities needed to quench the SCU increase as the current density is reduced. Near the critical current density of 1.43 kA/mm^2, the heat flux densities were about 1.3 mW/mm^2 and 0.5 mW/mm^2 for the cases of *SS* (or *Al*) and *SS**, respectively.

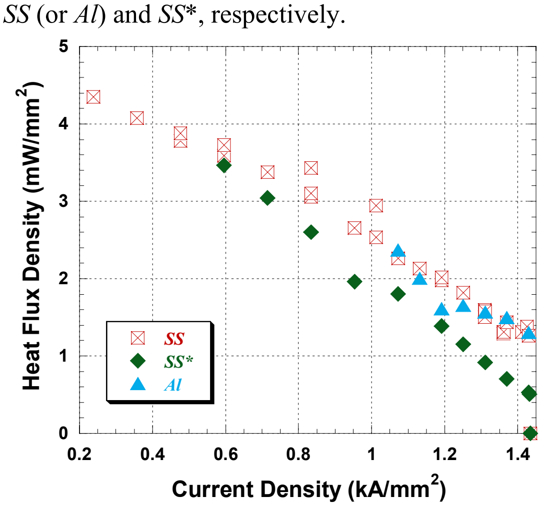

Figure 4: Steady-state heat loads to quench the SCU were measured as a function of the current density in 4.2 K pool-boiling LHe; *SS*: the thin film heater was attached inside a stainless-steel chamber as depicted in Fig. 3; *SS**: a thin layer of vacuum grease was applied between the SCU and the *SS* chamber to exclude any LHe at this interface; *Al*: an aluminum chamber was used instead of a stainless-steel one.

When LHe was excluded at the interface (*SS**), the vacuum chamber and the interface conducted away a heat flux of 0.5 mW/mm^2 so that it never reached the SC coil, as indicated by the heat flux near the critical current density at 0.998 j_c. When LHe was allowed into the interface (*SS* and *Al*), an additional 0.8 mW/mm^2 of heat flux density was carried away, making a total of 1.3 mW/mm^2. The results imply that LHe offers an efficient heat absorber for the SCU because of the relatively large latent heat of vaporization for LHe (2.6 mJ/mm^3).

The role of LHe is reasonably consistent with earlier work showing that, when a SC wire itself is the heat source, the quench energy increases by an order of magnitude from the wire enthalpy under transient conditions in pool-boiling LHe [3]. For the APS 7-GeV SR, the image current of the electron beam is the major source of dynamic heat load on the beam chamber except for the heat loads due to beam missteering and injection losses. At 4.2 K the power loss of the approximately 10-mm-wide image current from a 300 mA beam calculates to about 3.67 W/m [4]. This may be compared with the heat load of 10 W/m calculated from the above experimental data for the case without LHe at the interface or 26 W/m with LHe at the interface.

MAGNETIC FIELD MAPPING

The field B_y for the 22-period upper-half NbTi SCU was scanned using a Hall-probe mapping unit in a vertical dewar. During the measurements, the Hall probe was always in LHe. However, parts of the unit extended outside the dewar, and the probe was not calibrated at cryogenic temperatures. And, with only the upper-half SCU, the field perpendicular to the pole face is very sensitive to the distance between the probe and the coil/pole face of the SCU. Nevertheless, the mapping data would be very useful for modeling the end fields, shielding the coil terminal field and planning for correction coils.

Figure 5 (*top*) plots twice the undulator field for the upper-half unit at 800 A (0.935 kA/mm^2). The discrete data were scanned at a half pole gap of 3.6 mm, a scanning rate of about 10 mm/s with a field resolution of 1.2 G and a measurement interval of 0.2 mm. The total scanning distance was about 0.37 m. The pattern of coil turns per groove at the left end of the SCU is 3, 10, 17, 20; compared to 20 turns in the body of the SCU. At the right end, the pattern is 20, 10, 10, and 3 turns. The coil terminals, located near the end of the SCU for z > 0.3 m in Fig. 5, distorted the field shape.

From the first and second integrals of the vertical fields, the angles (*dx*/*dz*) and horizontal positions of the electron beams were calculated for the APS 7-GeV SR and are plotted in Fig. 5 (*bottom*), which shows that the fields for the left most 2/3 of the SCU are within a correctable range. More adjustment of the end field is still needed on the right side of the SCU.

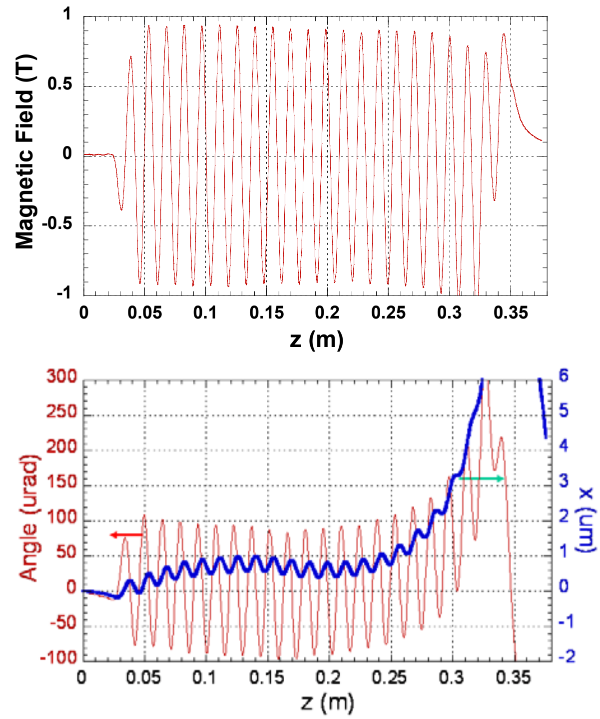

Figure 5: The field B_y for the upper-half SCUs was scanned at a distance of about 3.6 mm from the pole/coil surface (*top*). From the first and second integrals of the field, angles and positions of the electron beams are calculated (*bottom*).

ACKNOWLEDGMENTS

The authors thank K. Boerste for his assistance in SCU coil windings and test preparations.

REFERENCES

[1] S.H. Kim, C. Doose, R.L. Kustom, E.R. Moog and K.M. Thompson, "Design and Development of Short-Period Superconducting Undulator at the APS," ASC04, Jacksonville, Florida, Oct. 4 - 8, 2004.

[2] S.H. Kim, "A Scaling Law for the Magnetic Field Analysis of Superconducting Undulator," Nucl. Instrum. Methods A, accepted for publication.

[3] D.E. Baynham, V.W. Edwards and M.N. Wilson, "Transient Stability of High Current Density Superconducting Wires," IEEE Trans. Magn. **Mag -17** (1981) 732.

[4] R. L. Kustom, "Sources of Dynamic Heat Load for the Superconducting Undulator," unpublished data, 2004.